

Resolving the discrepancy between MOKE measurements at 1550-nm wavelength on Kagome Metal CsV_3Sb_5

Jingyuan Wang¹, Camron Farhang¹, Brenden R. Ortiz², Stephen D. Wilson² and Jing Xia¹

¹*Department of Physics and Astronomy, University of California, Irvine, CA 92697, USA*

²*Materials Department, University of California, Santa Barbara, Santa Barbara, CA 93106, USA*

Kagome metals AV_3Sb_5 ($\text{A} = \text{K}, \text{Cs}, \text{Rb}$) provide a rich platform for intertwined orders, where evidence for time-reversal symmetry breaking possibly due to the long-sought loop currents has emerged in μSR and MOKE experiments. Intriguingly, the observed spontaneous MOKE signals differ by orders of magnitude between different wavelengths, and more oddly, within the same wavelength. Here we perform comprehensive 1550 nm MOKE measurements on CsV_3Sb_5 under respective experimental conditions in prior reports. The results are consistent with Stanford and Irvine but differ in sign and size from Kyoto under identical conditions. The opposite behaviors of MOKE susceptibility under identical magnetic fields indicate different magnetic configurations between samples, which we conclude is the only remaining plausible explanation for the discrepancy in 1550 nm MOKE results.

Kagome metals featuring elaborate lattice structures and rich varieties of quantum phenomena have stimulated intense experimental efforts to uncover novel phases of matter where strong correlation and topological orders intertwine, such as in the case of Chern topological magnet TbMn_6Sn_6 [1]. The recently discovered quasi-two-dimensional Kagome compound family AV_3Sb_5 ($\text{A}=\text{K}, \text{Rb}$ and Cs) [2,3] is of great current interest due to its exhibition of charge density wave (CDW) [4–8], pressure-tunable superconductivity [3,9–12], and possibly time reversal symmetry breaking (TRSB) [13–15]. In particular, a TRSB order parameter in the CDW state has been reported in some of the muon-spin relaxation (μSR) [13–15] and magneto-optic Kerr effect (MOKE) [16–18] experiments, and may have connections with the long-sought loop currents [19,20] that were proposed for cuprate superconductors. AV_3Sb_5 's rich phase diagrams originate from the ideal Kagome network governed by layers of vanadium and antimony intercalated by alkali metal ions that crystallize in the $\text{p}6/\text{mmm}$ group [2,3]: tight-binding models of such Kagome lattices have revealed a fascinating electronic band structure containing Dirac cones, flat bands, and Van Hove singularities [3,21], making AV_3Sb_5 an interesting platform with intertwined [22] electronic instabilities for exotic correlated phases.

A hint for such an exotic phase in AV_3Sb_5 came from intriguing and seemingly contradicting MOKE experiments [16–18,23] that defy a unified explanation with existing theories including the loop currents model [20]. A spontaneous (without a magnetic field) MOKE [24,25] signal θ_K , which arises from the difference between refraction indices ($n + ik$) of time-reversed circularly polarized light beams, is a direct indication of TRSB. The majority of MOKE experiments have been conducted on the Cs compound CsV_3Sb_5 and have yielded disparate spontaneous θ_K values below the CDW transition temperature $T_{CDW} \sim 94 \text{ K}$, ranging from $450 \mu\text{rad}$ [17] and $50 \mu\text{rad}$ [16] at 800 nm wavelength, to $2 \mu\text{rad}$ [18] and

less than $0.03 \mu\text{rad}$ [23] at 1550 nm wavelength. Resolving these staggering discrepancies especially within the same wavelength is a prerequisite for understanding this intriguing Kagome metal. Since existing MOKE measurements [16–18,23] have been performed under rather different experimental conditions of magnetic field and thermal history [16–18,23], it is essential to first determine whether the discrepancy originates from different experimental conditions, or indicates distinct CDW states in CsV_3Sb_5 .

This paper focuses on 1550 nm because prior MOKE experiments at this wavelength [18,23] have been performed under extensive yet different experimental conditions using a similar Sagnac interferometry [26] technique, making direct comparisons possible. Here we have performed comprehensive 1550 nm MOKE measurements on a CsV_3Sb_5 sample, under respective experimental conditions used in [23] and [18]. The results are found to be condition-independent and are consistent with [23], but differ in size and sign from [18], hence ruling out experimental conditions as the cause for the discrepancy between [23] and [18]. In particular, we found *opposite* behaviors in the MOKE susceptibility (θ_K/B) across T_{CDW} between this work and [18] under *identical* magnetic fields and thermal ramp rates. This points to distinct magnetic configurations, which is plausible in CsV_3Sb_5 with intertwined [22] instabilities. Close examinations of the results rule out several proposed explanations for the discrepancy, and leave the multi-magnetic-state scenario as the only remaining plausible explanation for the contradiction between [23] and [18]. Implications and suggestions on reconciling the 800 nm MOKE experiments [16,17] will be discussed.

Before presenting our results, it's worthwhile to review some important details in the prior 1550 nm experiments [18,23]. They are all based on zero-loop Sagnac interferometry [26] that measures directly the optical phase difference between counterpropagating circularly polarized light beams. It is hence only sensitive to TRSB effects, and can achieve MOKE (θ_K) sensitivities of $\approx 0.01 \mu\text{rad}$ [26–

29]. A schematic of this interferometer is shown in Fig. 1(a), where time-reversed light beams in the polarization maintaining (PM) are converted by a quarter-wave plate (QWP) to opposite circular polarizations and interact with the sample during reflection. The returned light beams interfere at the detector and the MOKE signal θ_K is proportional to the ratio between the first harmonic power P_1 and the second harmonic power P_2 as explained in details in [26]. In a typical Sagnac experiment, θ_K is recorded first during cooldown with a magnetic field. The measured MOKE susceptibility θ_K/B gives a measure of magnetic susceptibility χ . In the subsequent zero field warmup (ZFW) spontaneous θ_K can be measured with TRSB domains aligned by the prior “training field” [18,23]. On CsV_3Sb_5 , the experiments performed at Stanford and Irvine [23] show no spontaneous θ_K with an uncertainty of $0.03 \mu\text{rad}$ after field trainings up to $0.03 T$ and $0.3 T$ respectively. In contrast, with much larger training fields up to $10 T$, the Kyoto experiment [18] using a Sagnac instrument constructed with assistance from the Irvine group has revealed below T_{CDW} a spontaneous $\theta_K \approx +2 \mu\text{rad}$ ($-2 \mu\text{rad}$) after positive (negative) field trainings. Equally puzzling is the opposite behaviors of MOKE susceptibility θ_K/B during field coolings. While θ_K/B decreases sharply below T_{CDW} in Stanford and Irvine experiments with lower magnetic fields [23] that agree with the sharp drop of magnetic susceptibility χ measured in similar samples [3], the Kyoto experiment at much larger fields [18] saw instead a sharp increase of θ_K/B below T_{CDW} .

This vast difference in the sizes of magnetic fields has been argued to be the most likely cause for the opposite behaviors in both θ_K/B and spontaneous θ_K between [23] and [18]. Indeed, metamagnetic phases with different magnetic configurations exist in strongly correlated materials such as those observed in the heavy Fermion metal CeAgBi_2 [30]. And the CDW states in AV_3Sb_5 is known to be tunable by magnetic fields [31–34]. Metamagnetic phases realized at different fields could exhibit opposite behaviors in θ_K/B below T_{CDW} . Consider the first order nature of the CDW transition, it is plausible that different zero-field ground states can be realized after removing the magnetic fields, yielding different spontaneous θ_K in [18,23].

The technical reason for the very different magnetic fields in [18,23] is due to different optical cryostats as illustrated in Fig. 1(a). The Stanford and Irvine experiments [23] were performed with the “ambient optics” setup (Fig. 1(a) left) with all optics outside the cryostat that was usually used for low field experiments [35,36]. The Kyoto experiment [18] was conducted with “cryo-optics” setup (Fig. 1(a) right) with QWP and lens inside the cryostat that was normally for high field experiments [37]. At zero magnetic field, there is no difference in measured θ_K between the two configurations. However, when a magnetic field is applied, the optical components in the magnetic field will have their own temperature-dependent contributes to θ_K via the Faraday effect, which need to be calibrated and removed to obtain

accurate readings of θ_K/B from sample. Such calibrations can only be performed properly with “ambient-optics” that are at fixed temperatures, as described in [23] for the calibration of the Irvine instrument. In contrast, due to the long thermalization time of glass at cryogenic temperatures, the individual temperatures of “cryo-optics” can deviate significantly from sample and are rather non-repeatable. These facts make signal subtraction with the “cryo-optics” setup such as in the Kyoto experiment [18] quite problematic. In this work we utilize both configurations, and we found that although the absolute value of θ_K/B can’t be obtained properly with the “cryo-optics” setup, the sharp change $\Delta\theta_K/B$ across T_{CDW} can be determined quite accurately in both setups.

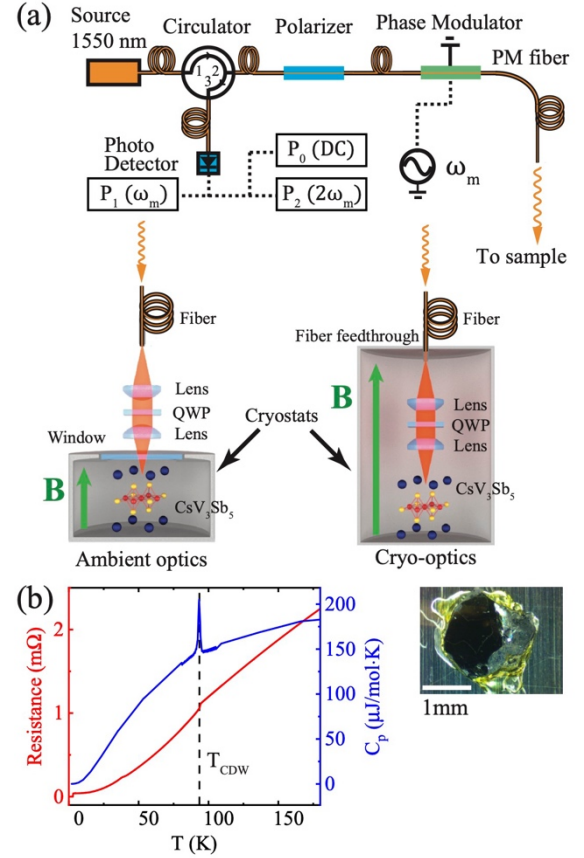


FIG. 1. Experimental configurations and CsV_3Sb_5 sample. (a) A Sagnac interferometer is connected to cryostats with either “ambient optics” (used in [23]) or “cryo-optics” (used in [18]). The “ambient optics” allow correct background removal in the presence of magnetic fields B , at the expense of limited size of B . (b) The CsV_3Sb_5 crystal used in this study with $T_{CDW} \sim 94 \text{ K}$ marked by a kink in the resistance, and a sharp peak in the specific heat C_p .

The high quality CsV_3Sb_5 single crystal (inset in Fig. 1(b)) used in this study is cut from the same piece as used in the prior Irvine experiment [23], and was grown by self-flux method at UCSB [3]. It is worth noting that the Kyoto experiment [18] used samples from a different group. The

first order CDW transition at $T_{CDW} \sim 94 K$ is clearly characterized by the sharp peak in the heat capacity C_p and a kink in the resistance as shown in Fig. 1(b). The crystal was then cleaved to expose optically flat areas and was mounted to both optical cryostats using Ge-varnish for minimal strain.

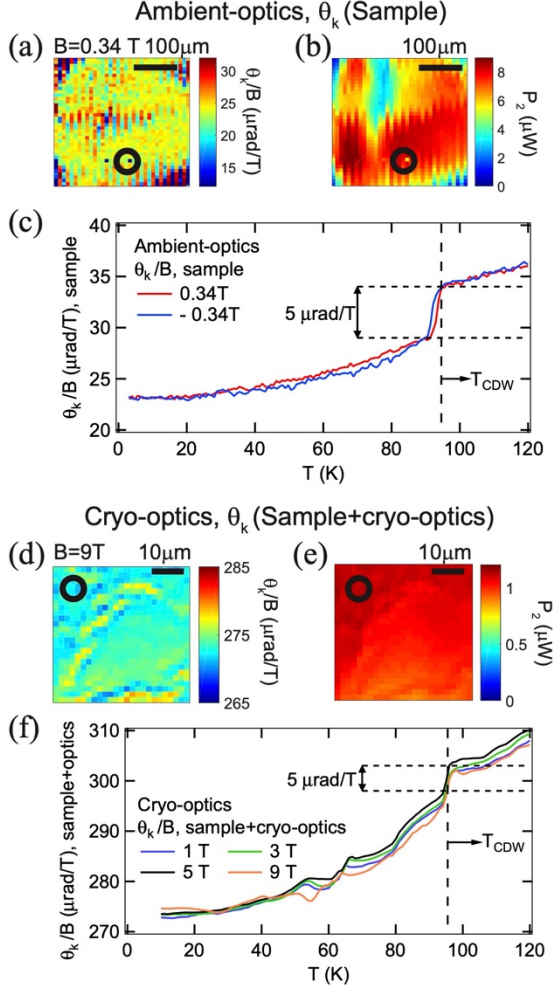


FIG. 2. In-field measurements with ambient-optics and cryo-optics setups plotted as θ_K/B . (a) and (b) are scanning images of θ_K/B and optical power P_2 in $B = 0.34 T$ at $T = 2 K$, showing uniform θ_K in optically flat regions ($P_2 > 2 \mu\text{W}$). (c) shows temperature dependence of θ_K/B in $B = \pm 0.34 T$ at a single point as circled in (a). The Faraday contribution from ambient optics is removed. (d), (e), (f) are corresponding data taken with the cryo-optics setup at higher magnetic fields, except that the Faraday contribution from cryo-optics (250 to 280 $\mu\text{rad}/T$) is not repeatable due to thermal lag and is not subtracted. In both low (c) and high fields (f), an abrupt decrease of $\Delta\theta_K/B \sim -5 \mu\text{rad}/T$ is evident below T_{CDW} .

We first present in-field measurements taken with either ambient-optics setup (Fig. 2(a)-(c)) or cryo-optics setup (Fig. 2(d)-(e)) to examine the behaviors of θ_K/B across T_{CDW} at different magnetic fields used in [18,23]. With both setups, we first perform spatial scans to locate optically flat regions, and then conduct temperature sweeps at a fixed point.

With the ambient-optics setup, the Faraday background ($-112 \mu\text{rad}/T$) has been calibrated [23] and removed. In Fig. 2(a) and (b), we present simultaneously taken scanning images of θ_K/B and optical power P_2 in $B = 0.34 T$ at $T = 2 K$, showing uniform $\theta_K/B \sim 24 \mu\text{rad}/T$ in optically flat regions with good reflection $P_2 > 2 \mu\text{W}$. Fig. 2(c) plots MOKE susceptibility θ_K/B during temperature sweeps in $B = \pm 0.34 T$ at a single point, which agree quantitatively with the data from Irvine experiment taken at identical fields [23]. The most prominent feature in $\Delta\theta_K/B$ is the sharp drop of $\Delta\theta_K/B \sim -5 \mu\text{rad}/T$ just below T_{CDW} from CDW transition. Due to the absence of a Curie-Weiss shape, we attribute θ_K/B to Pauli paramagnetism. And the sharp drop in θ_K/B below T_{CDW} can be explained by a decreased density of states below T_{CDW} . This agrees with the reported reduction of magnetic susceptibility χ in similar samples [3].

With the cryo-optics setup, the in-field measurements are extended to higher fields that were used in the Kyoto experiment [18]. Since Faraday backgrounds from cryo-optics can't be calibrated in temperature sweeps, they are not removed from the θ_K/B data presented in Fig. 2(d)-(e). Scanning images of θ_K/B (Fig. 2(d)) and optical power P_2 (Fig. 2(e)) were taken with $B = 9 T$ at $T = 2 K$, showing uniform $\theta_K/B \sim 274 \mu\text{rad}/T$ in the scanned region from sample and cryo-optics combined. Temperature sweeps of θ_K/B at a fixed location are plotted in Fig. 2(f) for $B = 1, 3, 5, 9 T$. They are clearly non-repeatable as the temperatures of cryo-optics and hence their Faraday contributions (250 to 280 $\mu\text{rad}/T$) do not repeat exactly due to thermal lag even with thermal ramp rates as slow as 0.3 K/minute. It is therefore unfeasible to extract the overall temperature dependence of θ_K/B with the cryo-optics setup as used in [18], except for the small temperature window near T_{CDW} where $\Delta\theta_K/B$ is dominated by the sample. Examine closely the sharp changes near T_{CDW} in Fig. 2(f), we found a consistent $\Delta\theta_K/B \sim -5 \mu\text{rad}/T$ for all applied high fields $B = 1, 3, 5, 9 T$, which fully agrees with the behaviors at $B = \pm 0.34 T$ discussed earlier, but is opposite in sign to $\Delta\theta_K/B \sim +7 \mu\text{rad}/T$ as reported in the Kyoto experiment at identical high fields [18]. Therefore it must be the sample, not the magnetic field, that has caused the opposite behaviors of $\Delta\theta_K/B$ between [18] and [23].

Next, we examine the spontaneous Kerr effect during zero magnetic field warmups (ZFW). The measurements were performed with the cryo-optics setup after cooldowns with identical magnetic fields and temperature ramping rates to the Kyoto experiment [18], and are presented in Fig. 3. Note that at zero field, there is no Faraday contribution from cryo-optics and hence θ_K is solely from the sample. A scanning image of spontaneous θ_K at $B = 0$ and $T = 2 K$ after 1 T training is presented in Fig. 3(a), and the simultaneously taken optical power image is presented in Fig. 3(b). There is no spontaneous θ_K through the scanned region with 1 μrad error bar, which is limited by the limited time spent at each pixel. More accurate measurements were taken at fixed

locations during very slow ZFW at 0.3 to 1 $K/minute$ ramp rates after trainings with $B = 1, 3, 5, 9 T$. The observed spontaneous θ_K during ZFW are presented in Fig. 3(c) in their raw form without any correction of drifts during the very long measurements. We observe no onset of any spontaneous θ_K below T_{CDW} with an uncertainty of 0.1 μrad . The larger uncertainty compared to [23] is due to larger drifts during longer experiments with such slow thermal ramp rates. And we conclude that magnetic field size is not the cause for the disparate reported θ_K values of $\pm 2 \mu rad$ at Kyoto [18] and $< 0.03 \mu rad$ at Stanford and Irvine [23].

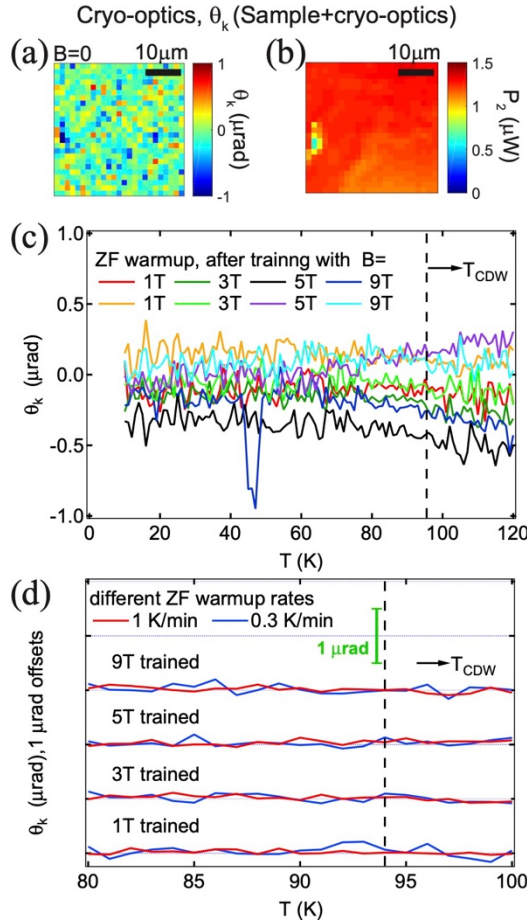


FIG. 3. Zero-field measurements with cryo-optics setup. No spontaneous θ_K was found below T_{CDW} with 0.1 μrad uncertainty. (a) and (b) are scanning images of θ_K and optical power P_2 at $B = 0$ and $T = 2 K$. (c) shows θ_K during ZFW after trainings with $B = 1, 3, 5, 9 T$ at a fixed point. (d) shows the ZFW with different thermal ramp rates of 1 K/min and 0.3 K/min , where traces are shifted by 1 μrad for clarity.

The exact CDW states in CsV_3Sb_5 , such as $2 \times 2 \times 2$ or $2 \times 2 \times 4$, could be affected by the speed of temperature ramping [4–7]. The Kyoto experiment [18] has used a much slower rate of 0.3 K/min compared to the 1 K/min rate used in the Stanford and Irvine experiments [23]. This

difference has been suggested as a necessary condition for observing the spontaneous MOKE signal at Kyoto [18] (private communications). To clarify this, we have performed ZFW measurements at both thermal ramp rates after training fields of $B = 1, 3, 5, 9 T$. The results are plotted in Fig. 3(d) with 1 μrad offsets between traces with different training fields for clarity. No spontaneous θ_K is found below T_{CDW} at either rate with an uncertainty of 0.1 μrad , ruling out thermal ramp rates as cause for contradictory 1550 nm MOKE experiments [18,23].

The comprehensive measurements presented so far have ruled out magnetic field or thermal ramp rate as the source for the discrepancy between MOKE experiments on CsV_3Sb_5 at 1550 nm [18,23]. There are only two remaining possibilities left. The first scenario is that the Sagnac instrument at Kyoto was calibrated incorrectly resulting in a wrong sign for the MOKE signal θ_K . In this case, the MOKE susceptibility θ_K/B at Kyoto [18] would in fact decrease below T_{CDW} , which agrees with Stanford and Irvine measurements [23] and this work. However, the spontaneous θ_K at zero field would also need to flip sign in the Kyoto experiment [18]: θ_K would be negative(positive) with positive(negative) training fields. This implies that the CDW state's spontaneous magnetic moment, possibly due to loop currents [20], is anti-aligned with the external training fields. There is no known mechanism for this anti-alignment, making this scenario highly unlikely.

The second and only remaining possibility is a multi-magnetic-state scenario, where the Kyoto sample has a different magnetic configuration in the CDW state, as indicated by their opposite behavior of $\Delta\theta_K/B$ across T_{CDW} even at identical magnetic fields and thermal ramp rates to this work. And different CDW ground states could lead to different spontaneous MOKE signals observed in different experiments. Multi-magnetic-states are plausible for AV_3Sb_5 with intertwined [22] instabilities where perturbations such as pressure is known to modify CDW state and superconductivity [9–12]. We note that this scenario may also explain the reported different TRSB onset temperatures and dynamic properties between μ SR experiments on CsV_3Sb_5 [13,15].

The two 800 nm MOKE experiments on CsV_3Sb_5 have both detected spontaneous MOKE signals but of very different magnitudes: $\theta_K \approx 450 \mu rad$ at PKU [17] and $50 \mu rad$ at Penn [16]. It is worth noting that similar samples have been used in the Penn and Irvine experiments, both report smaller MOKE signals in their respective wavelengths. This suggests that the large difference between PKU and Penn results both at 800 nm can be due to sample variations, which can be tested by in-field θ_K/B measurements across T_{CDW} . Finally, the spontaneous θ_K measured at 1550 nm [18,23] is one to four orders of magnitude smaller than those detected at 800 nm [16,17], necessarily requiring an unreported [38] resonance enhancement near 800 nm that would place constraints on the theoretical model of loop currents [20]. A definitive

clarification of this rather odd wavelength dependence requires MOKE experiments on the same sample at both wavelengths, which may be done with a Sagnac interferometer operating near 800 nm wavelength [39].

This project was supported mainly by the Gordon and Betty Moore Foundation through Grant GBMF10276, and in part by NSF award DMR-1807817. S.D.W. and B.R.O.

Email: xia.jing@uci.edu

References

[1] J.-X. Yin et al., *Quantum-Limit Chern Topological Magnetism in $TbMn_6Sn_6$* , *Nature* **583**, 533 (2020).

[2] B. R. Ortiz et al., *New Kagome Prototype Materials: Discovery of $KV3Sb_5$, $RbV3Sb_5$, and $CsV3Sb_5$* , *Phys. Rev. Materials* **3**, 094407 (2019).

[3] B. R. Ortiz et al., *$CsV3Sb_5$: A $Z2$ Topological Kagome Metal with a Superconducting Ground State*, *Phys. Rev. Lett.* **125**, 247002 (2020).

[4] Q. Stahl, D. Chen, T. Ritschel, C. Shekhar, E. Sadrollahi, M. C. Rahn, O. Ivashko, M. v. Zimmermann, C. Felser, and J. Geck, *Temperature-Driven Reorganization of Electronic Order in $CsV3Sb_5$* , *Phys. Rev. B* **105**, 195136 (2022).

[5] B. R. Ortiz, S. M. L. Teicher, L. Kautzsch, P. M. Sarte, N. Ratcliff, J. Harter, J. P. C. Ruff, R. Seshadri, and S. D. Wilson, *Fermi Surface Mapping and the Nature of Charge-Density-Wave Order in the Kagome Superconductor $CsV3Sb_5$* , *Phys. Rev. X* **11**, 041030 (2021).

[6] Z. Liang et al., *Three-Dimensional Charge Density Wave and Surface-Dependent Vortex-Core States in a Kagome Superconductor $CsV3Sb_5$* , *Phys. Rev. X* **11**, 031026 (2021).

[7] H. Li et al., *Observation of Unconventional Charge Density Wave without Acoustic Phonon Anomaly in Kagome Superconductors AV_3Sb_5 ($A=Rb, Cs$)*, *Phys. Rev. X* **11**, 031050 (2021).

[8] Q. Xiao, Y. Lin, Q. Li, X. Zheng, W. Xia, S. Zhang, Y. Guo, J. Feng, and Y. Peng, *Coexistence of Multiple Stacking Charge Density Waves in Kagome Superconductor $CsV3Sb_5$* , (2022).

[9] F. H. Yu, D. H. Ma, W. Z. Zhuo, S. Q. Liu, X. K. Wen, B. Lei, J. J. Ying, and X. H. Chen, *Unusual Competition of Superconductivity and Charge-Density-Wave State in a Compressed Topological Kagome Metal*, *Nat Commun* **12**, 3645 (2021).

[10] L. Zheng et al., *Emergent Charge Order in Pressurized Kagome Superconductor $CsV3Sb_5$* , *Nature* **611**, 682 (2022).

[11] F. Du, S. Luo, B. R. Ortiz, Y. Chen, W. Duan, D. Zhang, X. Lu, S. D. Wilson, Y. Song, and H. Yuan, *Pressure-Induced Double Superconducting Domes and Charge Instability in the Kagome Metal $KV3Sb_5$* , *Phys. Rev. B* **103**, L220504 (2021).

[12] N. N. Wang et al., *Competition between Charge-Density-Wave and Superconductivity in the Kagome Metal $RbV3Sb_5$* , *Phys. Rev. Research* **3**, 043018 (2021).

[13] R. Khasanov et al., *Time-Reversal Symmetry Broken by Charge Order in $CsV3Sb_5$* , *Phys. Rev. Research* **4**, 023244 (2022).

[14] C. Mielke et al., *Time-Reversal Symmetry-Breaking Charge Order in a Kagome Superconductor*, *Nature* **602**, 245 (2022).

[15] Z. Shan et al., *Muon Spin Relaxation Study of the Layered Kagome Superconductor $CsV3Sb_5$* , *Phys. Rev. Research* **4**, 033145 (2022).

[16] Y. Xu, Z. Ni, Y. Liu, B. R. Ortiz, Q. Deng, S. D. Wilson, B. Yan, L. Balents, and L. Wu, *Three-State Nematicity and Magneto-Optical Kerr Effect in the Charge Density Waves in Kagome Superconductors*, *Nat. Phys.* **18**, 1470–1475 (2022).

[17] Q. Wu et al., *Simultaneous Formation of Two-Fold Rotation Symmetry with Charge Order in the Kagome Superconductor $CsV3Sb_5$ by Optical Polarization Rotation Measurement*, *Phys. Rev. B* **106**, 205109 (2022).

[18] Y. Hu et al., *Time-Reversal Symmetry Breaking in Charge Density Wave of $CsV3Sb_5$ Detected by Polar Kerr Effect*, *arXiv:2208.08036*.

[19] F. D. M. Haldane, *Model for a Quantum Hall Effect without Landau Levels: Condensed-Matter Realization of the “Parity Anomaly,”* *Physical Review Letters* **61**, 2015 (1988).

[20] C. M. Varma, *Non-Fermi-Liquid States and Pairing Instability of a General Model of Copper Oxide Metals*, *Phys. Rev. B* **55**, 14554 (1997).

[21] M. Kang et al., *Twofold van Hove Singularity and Origin of Charge Order in Topological Kagome Superconductor $CsV3Sb_5$* , *Nat. Phys.* **18**, 301 (2022).

[22] E. Fradkin, S. A. Kivelson, and J. M. Tranquada, *Colloquium : Theory of Intertwined Orders in High Temperature Superconductors*, *Rev. Mod. Phys.* **87**, 457 (2015).

[23] D. R. Saykin et al., *High Resolution Polar Kerr Effect Studies of $CsV3Sb_5$: Tests for Time Reversal Symmetry Breaking Below the Charge Order Transition*, *arXiv:2209.10570*.

[24] S. D. Bader, *Smoke*, *Journal of Magnetism and Magnetic Materials* **100**, 440 (1991).

[25] Z. Qiu, *Surface Magneto-Optic Kerr Effect (SMOKE)*, *Journal of Magnetism and Magnetic Materials* **200**, 664 (1999).

[26] J. Xia, P. T. Beyersdorf, M. M. Fejer, and A. Kapitulnik, *Modified Sagnac Interferometer for High-*

acknowledge support via the UC Santa Barbara NSF Quantum Foundry funded via the Q-AMASE-i program under award DMR-1906325.

Sensitivity Magneto-Optic Measurements at Cryogenic Temperatures, *Appl Phys Lett* **89**, 062508 (2006).

- [27] E. R. Schemm, W. J. Gannon, C. M. Wishne, W. P. Halperin, and A. Kapitulnik, *Observation of Broken Time-Reversal Symmetry in the Heavy-Fermion Superconductor UPt3*, *Science* **345**, 190 (2014).
- [28] X. Gong, M. Kargarian, A. Stern, D. Yue, H. Zhou, X. Jin, V. M. Galitski, V. M. Yakovenko, and J. Xia, *Time-Reversal Symmetry-Breaking Superconductivity in Epitaxial Bismuth/Nickel Bilayers*, *Sci. Adv.* **3**, e1602579 (2017).
- [29] I. M. Hayes et al., *Multicomponent Superconducting Order Parameter in UTe2*, *Science* **373**, 797 (2021).
- [30] S. M. Thomas, P. F. S. Rosa, S. B. Lee, S. A. Parameswaran, Z. Fisk, and J. Xia, *Hall Effect Anomaly and Low-Temperature Metamagnetism in the Kondo Compound CeAgBi 2*, *Phys. Rev. B* **93**, 075149 (2016).
- [31] Y.-X. Jiang et al., *Unconventional Chiral Charge Order in Kagome Superconductor KV3Sb5*, *Nat. Mater.* **20**, 1353 (2021).
- [32] N. Shumiya et al., *Intrinsic Nature of Chiral Charge Order in the Kagome Superconductor RbV3Sb5*, *Phys. Rev. B* **104**, 035131 (2021).
- [33] Z. Wang et al., *Electronic Nature of Chiral Charge Order in the Kagome Superconductor CsV3Sb5*, *Phys. Rev. B* **104**, 075148 (2021).
- [34] E. van Heumen, *Kagome Lattices with Chiral Charge Density*, *Nat. Mater.* **20**, 1308 (2021).
- [35] S. Thomas et al., *Localized Control of Curie Temperature in Perovskite Oxide Film by Capping-Layer-Induced Octahedral Distortion*, *Phys. Rev. Lett.* **119**, 177203 (2017).
- [36] C. Gong et al., *Discovery of Intrinsic Ferromagnetism in Two-Dimensional van Der Waals Crystals*, *Nature* **546**, 265 (2017).
- [37] J. Xia et al., *Polar Kerr-Effect Measurements of the High-Temperature $YBa_2Cu_3O_6+x$ Superconductor: Evidence for Broken Symmetry near the Pseudogap Temperature*, *Phys. Rev. Lett.* **100**, 127002 (2008).
- [38] E. Uykur, B. R. Ortiz, O. Iakutkina, M. Wenzel, S. D. Wilson, M. Dressel, and A. A. Tsirlin, *Low-Energy Optical Properties of the Non-Magnetic Kagome Metal CsV3Sb5*, *Phys. Rev. B* **104**, 045130 (2021).
- [39] A. Fried, M. Fejer, and A. Kapitulnik, *A Scanning, All-Fiber Sagnac Interferometer for High Resolution Magneto-Optic Measurements at 820 nm*, *Review of Scientific Instruments* **85**, 103707 (2014).